

Contribution of higher-order structure to perception of mirror symmetry: Role of shapes and corners

Cayla A. Bellagarda

School of Psychological Science, University of Western
Australia, Crawley, Western Australia



J. Edwin Dickinson

School of Psychological Science, University of Western
Australia, Crawley, Western Australia



Jason Bell

School of Psychological Science, University of Western
Australia, Crawley, Western Australia



David R. Badcock

School of Psychological Science, University of Western
Australia, Crawley, Western Australia



Visual mirror symmetry is a global feature that is dependent on specific low-level relationships between component elements. Initially conceptualized as virtual lines between paired elements, it has been suggested that higher-order structure between pairs of symmetric elements forming virtual four cornered shapes may also be important for strengthening the percept of mirror symmetry. We utilize corner elements, formed by joining two Gabor elements along a central midline creating vertices with variable internal angles, in a temporal integration paradigm. This allows us to specifically manipulate the presence and type of higher-order versus lower-order structure in patterns with symmetrically placed elements. We show a significant contribution of higher-order structure to the salience of visual symmetries compared with patterns with only lower-order structures. We also find that although we are more sensitive to patterns with higher-order structure, there is no difference in the temporal processing of higher-order versus lower-order patterns. These findings have important implications for existing spatial filter models of symmetry perception that rely on lower-order structures alone and reinforces the need for elaborated models that can more readily capture the complexities of real-world symmetries.

Introduction

Whereas symmetry itself is an inherently global percept, it is derived from very precise relationships between local information. In other words, although symmetry is a descriptor of a higher-level structure

of a pattern or object, it is dependent on low-level relationships between components. This means that minor alterations to the positioning or appearance of individual local features can have a disruptive effect on the salience of the global symmetry. Changes in luminance polarity (Bellagarda, Dickinson, Bell, & Badcock, 2021; Mancini, Sally, & Gurnsey, 2005; Wenderoth, 1996; Zhang & Gerbino, 1992), element orientation (Locher & Wagemans, 1993; Saarinen & Levi, 2000), color (Gheorghiu, Kingdom, Remkes, Li, & Rainville, 2016; Morales & Pashler, 1999), and positional skewing (Sawada & Pizlo, 2008; Wagemans, 1993; Wagemans, van Gool, & d'Ydewalle, 1991) have all been shown to affect the perception of symmetry. Alterations of global features, such as the orientation of the symmetric axis (Corballis & Roldan, 1975) or pattern outline (Wenderoth, 1995), can also change the way patterns with otherwise identical local symmetry information are perceived.

Sensitivity to symmetry is thought to have arisen in the visual system because it often identifies an object, which is the predominant role of form perception systems (Locher & Nodine, 1989). Symmetry is considered a non-accidental property, because it is highly unlikely to occur in a visual image by chance if it is not present in the physical object (Barlow, 1985; Baylis & Driver, 1995). Symmetry is therefore a useful way of segregating objects from their background (Driver, Baylis, & Rafal, 1992). It has also been argued to be a signifier of genetic quality (Jones, Little, Penton-Voak, Tiddeman, Burt, & Perrett, 2001; Simmons, Rhodes, Peters, & Koehler, 2004), object affordance or utility (Treder, 2010), and aesthetics

Citation: Bellagarda, C. A., Dickinson, J. E., Bell, J., & Badcock, D. R. (2023). Contribution of higher-order structure to perception of mirror symmetry: Role of shapes and corners. *Journal of Vision*, 23(1):4, 1–18, <https://doi.org/10.1167/jov.23.1.4>.



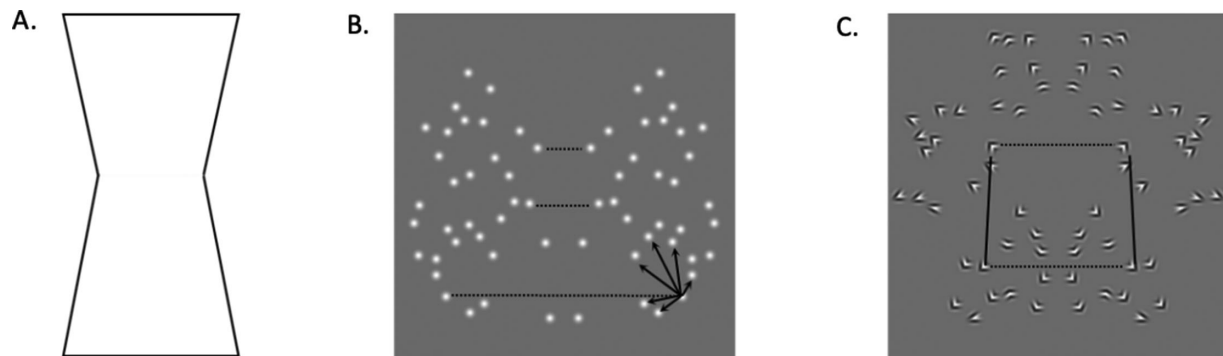


Figure 1. Examples of symmetric stimuli with differing higher and lower-order structures including (A) a solid polygon with only high-order structure, (B) dot patterns with lower-order structure, and (C) patterns from the current study, where corner elements allow manipulation of both higher- and lower-order structure. Virtual lines dictated by element position are shown with solid lines. Potential projected lines are shown by solid lines. Lower order structure is defined as pairwise virtual lines spanning the symmetry axis, shown by broken lines between paired elements. Higher-order structure is highlighted by solid lines on the same side of the axis. In the A solid polygon stimuli, the higher-order structure may be necessary for symmetry perception as well as there is some lower-order symmetry information conveyed by the corresponding points on the lines and corners, there is a paucity of discrete virtual or projected lines. Therefore, symmetry perception based on lower-order processing alone (e.g. spatial filtering) will be possible but is likely to include more noise. It is also difficult to manipulate higher or lower order structure in isolation; often these shapes are 100% symmetric or 100% asymmetric. In B, symmetry is defined by virtual lines between dot elements at equivalent positions over the axis. Although there may be some incidental groupings on the same side of the axis, any one dot is equally likely to co-align with any other dot and could produce infinite spurious projected lines, shown by the arrows in Figure 1B, meaning that this incidental higher-order structure is not a useful cue. In C, both higher and lower-order structure is explicitly manipulated by varying the coalignment of angled elements. Virtual lines within element pairs (lower-order structure, dotted lines) and projected lines between element pairs (higher-order-structure, solid lines) are defined to form intermediate structures between individual local dot pairings and the global symmetric pattern.

(Locher & Nodine, 1989). Further, it has recently been shown that symmetry specific neural responses are generated when viewing symmetric real-world stimuli, such as flowers or landscapes (Makin, Rampone, Karakashevska, & Bertamini, 2020). The magnitude of this response scales with the quality of the figural symmetry, but to a lesser extent for symmetry of background landscape details (Makin et al., 2020). Inspired by the idea that symmetry is an object cue, some researchers have used irregular polygons as stimuli (see Figure 1A for an example). Generally, these stimuli are composed of two irregular contours (i.e. lines with variable type and number of convexities and/or concavities along their length) joined by two straight lines forming the top and bottom edge of the shape (Baylis & Driver, 1995; Baylis & Driver, 2001). By manipulating the angles at the corners of these contours and the positioning of the top and bottom lines, the contours can either be reflected or translated, and can be made to appear as part of one shape or split across two shapes (Baylis & Driver, 1995; Bertamini, 2010). Pashler (1990) argues that the functional purpose of symmetry stems from its ability to convey information about the orientation of an object. Therefore, symmetry is an important reference point in the case of distortion due to observer viewpoint or image plane. The use of solid polygons to investigate symmetry perception

appears logical if considering symmetry as signaling a meaningful figure against a ground (Baylis & Driver, 2001; Bertamini, 2010; Friedenborg & Bertamini, 2000; Pashler, 1990) and provides important support for the role of symmetry in structuring the visual world. However, the utility of solid polygons is restricted to investigating global features of symmetry, as their local structural information cannot be readily manipulated in a manner that changes the global percept (Machilsen, Pauwels, & Wagemans, 2009).

Although solid polygons have been useful for considering the role of symmetry as a figural cue, far more popular in the symmetry perception literature more broadly are sparse dot patterns or patterns composed of Gabor patches. Dot and Gabor patterns allow for the independent manipulation of global factors, such as symmetry axis orientation, as well as local factors at the element level (e.g. element luminance polarity or element orientation). Whereas sparse element patterns do not appear to readily permit investigation of structure, early Gestalt theorists argued that symmetry was a grouping principle, and is considered an extension of the laws of good continuation and proximity (Machilsen et al., 2009). That is, symmetry is dependent on very specific arrangements of local information that convey an impression of structure in an otherwise abstract pattern

(Jenkins, 1983). The component process model of Jenkins (1983) is an early attempt to operationalize the lower order structural relationships that lead to the percept of symmetry. The accompanying model has three main components; detection of the orientational uniformity that establishes symmetric pairs, fusion of these elements into a salient “virtual line,” and detection of global symmetry from the coalignment of the midpoint of these pairs/virtual lines along a symmetry axis. The concept of virtual lines is not unique to Jenkins’ (1983) model, having been previously referred to as chords by Moor and Parker (1974) or dipoles by Julesz (1971). In the case of mirror symmetry, such virtual lines define pairwise groupings of elements orthogonally across an axis to create lower-order structure (see Figure 1B). Virtual lines formed by elements running orthogonally to a symmetry axis are fundamental to definitions of mirror symmetry and are reflected in influential spatial filter models (Cohen & Zaidi, 2013; Dakin & Hess, 1997; Dakin & Watt, 1994; Rainville & Kingdom, 2000). Virtual lines in this conceptualization is specific to the line orthogonal to the symmetry axis between the position of element one and element two. When elements are symmetrically positioned, these lines will be uniformly straight and orthogonal relative to the symmetry axis. Although pairwise positional groupings along these virtual lines are generally thought to be necessary for symmetry perception in dot patterns (Jenkins, 1983). Wagemans and colleagues (Wagemans, 1993; Wagemans, van Gool, Swinnen, & Horebeek, 1993; Wagemans, van Gool, & d’Ydewalle, 1991) point out that this lower order structure can be augmented by additional information making it more resistant to noise.

In particular (Wagemans & colleagues, 1993; Wagemans et al., 1993; Wagemans et al., 1991) were interested in the idea of skewed symmetry. In skewed symmetry, lower-order structure according to Jenkins (1983), specifically midpoint collinearity and orientational uniformity of the virtual lines between elements is retained, but these are not perfectly orthogonal to the symmetry axis. In this case, participants find it significantly more difficult to perceive skewed symmetry compared to non-skewed symmetric patterns (Wagemans, 1993; Wagemans et al., 1991). However, Wagemans et al. also observed that skewing was much less disruptive when patterns had multiple symmetry axes compared to single axis patterns (Wagemans et al., 1991). Wagemans and colleagues postulated that this occurs because of the presence of high-level structure in these patterns, and this led them to develop what they termed the correlational quadrangle or bootstrap model of mirror symmetry (Wagemans et al., 1993). Here, the concept of lower-order pairwise grouping of elements is retained, but this is bolstered by additional structure introduced by pairs of pairwise groupings. These “pairs of pairs”

form four-sided virtual polygons that can be either reflected over the axis (two discrete reflected shapes) or one larger shape spanning the symmetry axis (a correlational quadrangle). An example of this is shown in Figure 1C. Symmetry signal is strongest when the angles formed within these paired virtual lines form a well-defined symmetric trapezoid or parallelogram. When these higher-order correlations are present, global symmetry is more readily apparent from the explicit lower-order dot pairings (Wagemans et al., 1993). The propagation of a local reference frame from individual elements and element pairs (Pashler, 1990) is facilitated by the additional structure as it provides additional cues for the most likely, or most informative, direction for this reference frame to proceed. This process is referred to as bootstrapping by Wagemans et al. (1993), and is argued to be the mechanism by which local regularity and global symmetry is reconciled in the visual system. This is supported by Wagemans et al. (1993) finding that patterns with global regularity (i.e. where dot elements were grouped or positioned to form parallelograms or trapezoids) were more readily detected and less affected by skewing than patterns defined by lower-order pairs alone. This model has also been applied to patterns with multiple axes of symmetry, albeit with varying results (Treder, van der Vloed, & van der Helm, 2011; Wagemans et al., 1991).

One limitation to testing (Wagemans et al., 1993; Wagemans et al., 1991) correlational quadrangle model, however, is that their stimuli were restricted to dot patterns. As mentioned previously, local information in dot patterns is non-oriented and therefore virtual lines can be drawn in any direction from a given dot to coincide with any other dot in the array, which can also occur in the solid polygon stimuli. In their experiments (Wagemans & colleagues, 1993; Wagemans, 1993; Wagemans et al., 1991) varied the presence and type of lower- and higher-order structure by manipulating the placement of each dot relative to the other dots in an array. For example, this could include ensuring optimum collinearity among four dots (or two symmetric pairs) to form quadrangles spanning the width of the pattern or grouping four elements in close proximity on one side of the axis and reflecting this over the axis. Although it is assumed that these manipulations are sufficient to create or destroy a given intermediate structure, the non-oriented nature of dots mean that there is no way to explicitly prevent or discourage interconnections between elements and spurious groupings or virtual lines are likely. Gabor elements with a narrow orientation bandwidth have been utilized in symmetry perception research (Koeppel & Morgan, 1993; Locher & Wagemans, 1993; Saarinen & Levi, 2000; Sharman & Gheorghiu, 2019), but have similar limitations to dots when attempting to manipulate higher-order structural relationships. That is, each Gabor in a symmetric array only conveys

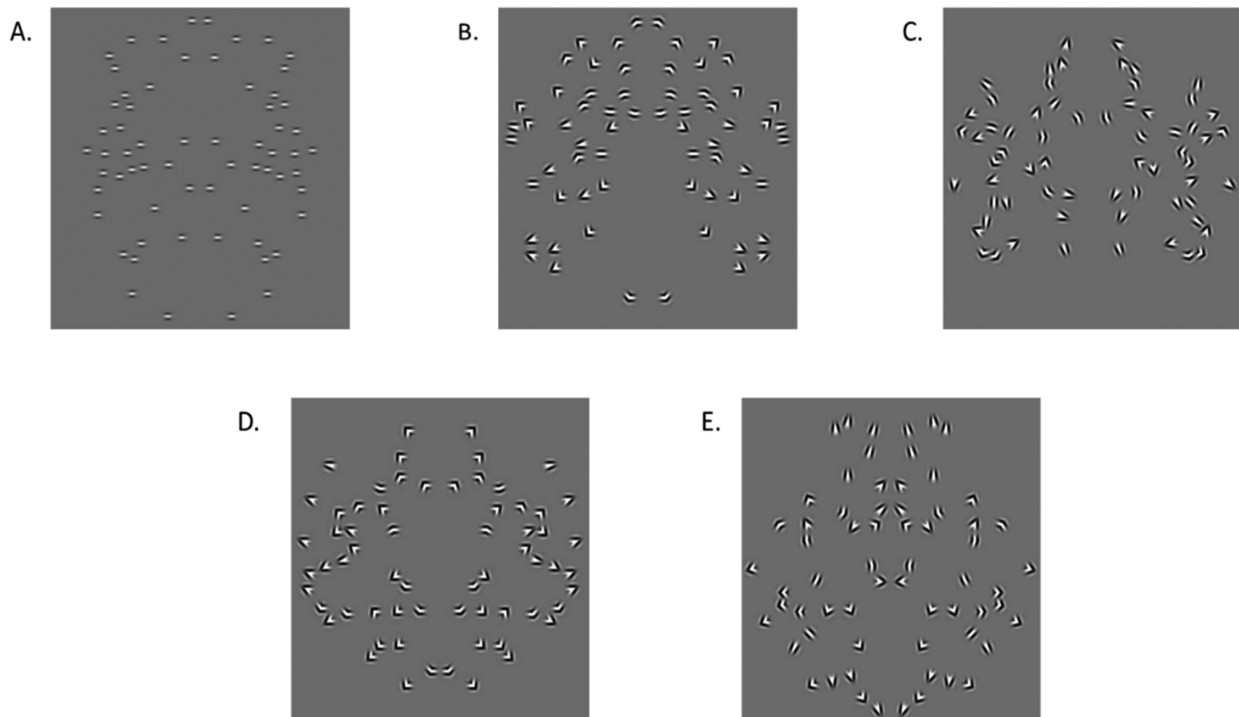


Figure 2. Examples of the five symmetry conditions used in the current study. In the top row, signal is defined by paired elements, either (A) horizontal Gabors, (B) mirrored corners, or (C) unmirrored corners where symmetry is identifiable by position only. The two conditions in the bottom row both have higher-order structure defined by groups of elements, either (E) shapes mirrored across the axis, or (D) correlational quadrangles. In these two cases, vertices are mirrored across the symmetric axis but the nature of the shape comparison differs. In D correlational quadrangles, the shapes cross the symmetric axis, whereas in E reflected shapes they do not, but shape pairs themselves are symmetric. See Figure 6 for examples where the mirrored shapes and correlational quadrangles are highlighted on the image.

one dominant orientation (e.g. they can be either horizontal or vertical, but not both), and therefore promote projected lines continuing along this dominant orientation only. Where virtual lines are dictated by element position (Jenkins, 1983), projected lines here instead refer to the continuation of an implied contour along the trajectory signaled by the orientation of an element. For example, in the case of symmetrically positioned vertical Gabor's, there are horizontal virtual lines between paired elements, and vertical projected lines implied by the orientation of the individual Gabors. Dot patterns have the same virtual lines as Gabor patterns, but do not have constrained projected lines. Based on the principles of good continuation, it has been shown that Gabor elements sharing a similar projected line can form continuous contours which, like symmetric virtual lines, conveys a sense of structure and readily segments signal from noise (Field, Hayes, & Hess, 1993; Li & Gilbert, 2002; Tan, Dickinson, & Badcock, 2016). However, because individual Gabors can only convey one dominant projected line, and symmetry is defined by specific arrangements of virtual lines, inter-connections between elements not falling

along these dominant virtual and projected lines cannot be easily manipulated.

An alternative element type that is potentially better suited to this task was recently developed by (Persike & Meinhardt, 2016; Persike & Meinhardt, 2017) in their investigation of the role of corners in contour integration. Their corner elements were formed by joining two Gabor elements and contained two different orientation components (see Figures 1 and 2 for examples where corners are included in symmetric arrays, and Figure 3 for discrete examples of the different corners). In their subsequent experiments, they found that contours could be formed using corner elements alone (i.e. without intermediate elements) without detrimental effect on contour perception. Contours were formed by grouping several corner elements such that the orientation component (or leg) of each element coaligned with the adjacent leg of the next element, such that they fell on the trajectory of the same projected line. We suggest (Persike & Meinhardt, 2016; Persike & Meinhardt, 2017) corner elements provide a method for nuanced manipulation of higher- and lower-order structure in visual mirror

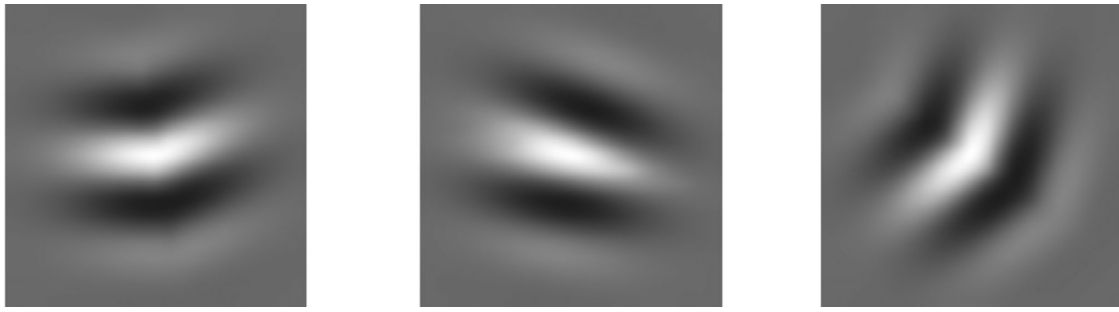


Figure 3. Examples of corner elements with different internal angles. Each one is made of two halves of Gabor elements joined along the line bisecting the vertex.

symmetry perception. By varying the alignment of the two component Gabors, legs, of symmetrically placed corner elements, we can explicitly manipulate the presence and type of both higher- and lower-order structure within the pattern by introducing projected lines in two directions from the same element. This eliminates the confounding relationships between elements present in (Wagemans' & colleagues, 1993; Wagemans, 1993; Wagemans et al., 1991) earlier investigations and allows for both virtual lines within- and projected lines between-element pairs to be made more explicit and independently manipulated in multiple directions simultaneously. This introduction of two projected lines per element therefore allows us to build on the structure implied by virtual lines between paired elements alone.

Our experiment has two complimentary aims; (1) to investigate how corner elements interact with global mirror symmetry, extending (Periske & Meinhardt's, 2016; Periske & Meinhardt, 2017) contour integration research, and (2) providing a more controlled exploration of the role of higher-order structure in mirror symmetry perception to build on (Wagemans & colleagues, 1993; Wagemans, 1993; Wagemans et al., 1991) correlational quadrangle model. We use a temporal integration paradigm to compare both sensitivity and temporal processing of discrete symmetric patterns composed of either individual Gabor elements or corner elements. To do so, we use the same temporal integration paradigm used in Bellagarda, Dickinson, Bell, and Badcock (2022) in which a temporal onset asynchrony is introduced between the elements of a symmetric pair. This method allows the consideration of both sensitivity to a particular stimulus and also the time window over which it acts as a symmetry signal for the visual system. Our previous work, particularly Bellagarda et al. (2022), has shown that symmetric patterns to which we are equally sensitive can have different visible persistences (Bellagarda et al., 2021; Niimi, Watanabe, & Yokosawa, 2005), and patterns that have the same estimated

duration of visible persistence can have different detection thresholds. By considering both sensitivity (detection thresholds) and temporal processing (visible persistence), we are better able to consider potential underlying mechanisms and detect subtle differences between conditions that could appear equivalent if only examining sensitivity in isolation. Shown in Figure 2 our conditions are similar to those used by Wagemans et al. (1993), in that symmetry can be defined by horizontal virtual lines only (lower-order structure), correlational quadrangles (four sided trapezoids, marked only by their corners, spanning the entire width of the pattern), or reflected shapes (groups of four elements reflected over the axis). However, Wagemans et al. (1993) stimuli were restricted to manipulation of element position only, thereby making their higher-order structure implicit and reliant on grouping elements (specifically pairs of pairs). Using discrete corner elements allows for higher-order structure to be made explicit, and the relationships between elements (and element pairs) to be precisely defined based on the good continuation of the projected lines of the coaligned legs, which facilitates explicitly manipulated interactions between some elements and not others while maintaining positional symmetry.

Stimuli for three of our specific conditions contain only lower-order structure defined by element position and orientation (e.g. mirrored, see Figure 2B, or unmirrored corners, see Figure 2C, and horizontal Gabors, see Figure 2A). A further two conditions contained higher-order structure through coalignment of both legs of each element to explicitly create pairs of paired elements joined by coincident projected lines, and therefore virtual parallelograms defined by four coaligned corners (see Figures 2D,E). A detailed description for each condition in turn is provided below. We hypothesize that patterns with corner elements will be as readily perceptible as patterns with Gabor elements only, as long as the corners are reflected over the midline. If there is no coalignment of either leg of an element, symmetry should be less salient as the

fundamental projected lines are disrupted even though the element position and therefore the virtual lines are still symmetric, similar to findings with Gabors of unmirrored orientations. We also hypothesize that addition of higher-order structure (virtual polygons) should improve symmetry perception relative to patterns with lower-order structure alone, consistent with findings by [Wagemans et al. \(1993\)](#). By using corner elements, we can explicitly manipulate type of higher order structure present by controlling element alignment for each part of a corner element. More importantly, we are also able to directly control the number of correlational quadrangles present, as each corner can only interact with a finite number of other elements in a specified manner. In this way we can more directly test the limits of [Wagemans et al. \(1993\)](#) hypotheses and provide a systematic comparison from lower-order structure and Gabors only, through to different types of higher-order structures. A temporal integration paradigm allows us to also consider potential underlying mechanisms, and whether these may differ between higher- and lower-order structures.

Method

Participants

Four participants (one female, range 24 to 56 years) completed all experimental conditions. All participants had normal or corrected to normal visual acuity. One participant has a divergent squint and viewed the stimuli monocularly as their left eye was patched. The research was approved by the Human Research Ethics committee at the University of Western Australia and conformed to the tenets of the Declaration of Helsinki. Informed consent was obtained from all participants. The participants were experienced observers who have completed other similar experiments.

Apparatus

All stimuli were generated using Matlab version 7.0 (Mathworks, Natick, MA, USA) and presented on a Sony Triton G520 monitor (screen resolution 1024 × 768 pixels, refresh rate 100 Hz) via a Cambridge Research Systems (CRS) ViSaGe (CRS, Kent, UK) visual stimulus generator. Each pixel subtends two inches of visual angle at the viewing distance of 65.5 cm which was stabilized by a chin rest. Participants made their responses via a CRS, CB6 button box.

General stimulus features

Each stimulus was composed of 64 discrete elements placed within a circular window of 6.4 degrees radius

on a uniform grey background (luminance 45 cd/m², CIE1931xy coordinates 0.327, 0.347). To prevent overlap, each element was restricted from falling within 30 inches of any other element. The centers were also restricted from falling within 20 inches of the window's border so that their contrast relative to the background would be imperceptible beyond the window. Elements also could not fall within 15 inches of the central axis of the pattern, meaning there was a slight reduction in density along this region in both symmetric and non-symmetric patterns. Both signal and reference stimuli had the same space-averaged element density, within the window, of 0.49 elements/deg².

Constructing vertices

Each element in the array was composed of two spatially coincident Gabor patches, sinusoidal gratings within a window with a Gaussian contrast profile, angled to create a vertex, examples of which are presented in [Figure 3](#). For each individual Gabor, the standard deviation of the Gaussian window of each patch was 8 inches of visual angle, with a full width of the envelope at half maximum of 18.84 inches. The spatial frequency of the grating was four cycles per degree of visual angle, and carriers were in cosine phase. At their maximum luminance point, the Gabors were twice as bright as the background (Weber contrast 1). Once the orientation of the edges comprising the vertex were defined, the Gabor patches were then halved. These halves were re-joined along the line bisecting the internal angle of the vertex. The nature of these vertices and the way their internal angle was defined depended on the stimulus condition and they were determined by the shapes required in the stimuli.

The Method of Constant Stimuli (MOCS) was used to collect data corresponding to a range of signal to noise ratios for each stimulus. Each symmetric signal pattern could have four, eight, 12, 16, 20, 24, 28, or 32 pairs of symmetrically positioned vertices out of a total of 32 possible pairs (in this case, 32 pairs equals 100% symmetry). In conditions where signal was defined by symmetric shapes the shapes were comprised of four vertices each. Positions for half of the total signal elements on a given trial were selected on one side of an implied central vertical axis, and then reflected over this central midline to form a mirror symmetric pair. The remaining elements were unpaired noise elements, meaning that no other element was spatially coincident with them across the axis. In both the noise elements of the signal stimuli, and the non-symmetric reference stimuli, the total number of required noise elements required were positioned on one side of the axis and then reflected. This means that twice as many element locations as required were selected. One half of the noise elements were randomly selected and

removed, one from each mirrored pair. This means that the intended signal to noise ratio (or total number of elements in the case of the asymmetric reference pattern) was retained, and any accidental symmetry pairings were precluded. In this manner, an equal number of signal elements were present on both sides of the axis in all stimuli. On average, signal and noise elements were the same distance from the symmetry axis.

Temporal delay conditions

All stimuli were dynamic and included an intra-pair temporal delay varying between 0 ms and 60 ms. Each stimulus was composed of 32×10 ms frames, and each element had a lifetime of 40 ms (or four frames). Each element in the array was temporally offset relative to its symmetrically positioned partner, using a similar paradigm to our previous temporal integration studies (Bellagarda et al., 2021). The duration of this delay varied between 0 ms and 60 ms, in 10 ms steps (or one frame). Previous studies have consistently identified 60 ms as the upper temporal limit over which mirror symmetry can be integrated and perceived in most cases (Bellagarda et al., 2021; Hogben, Julesz, & Ross, 1976; Niimi et al., 2005; Sharman, Gregersen, & Gheorghiu, 2018) so intra-element delays beyond 60 ms were not considered in this experiment. On each frame, a quarter of the total elements were removed and replaced with new elements in a new location. In all conditions other than 0 ms delay, the generation of signal elements on the right side of the axis was delayed by a defined number of frames relative to their partner on the left side of the axis. The generation of the second element in each pair via the process described above was therefore delayed by between zero and six frames relative to their partner.

Lifetimes of positionally symmetric elements temporally overlapped for a portion of time if the delay was less than 40 ms because delay durations are measured from the onset of element one in the pair to the onset of element two (a stimulus onset asynchrony, or SOA). This means that a portion of the symmetrically positioned elements in a pattern will have a mirrored partner physically present on the screen for one, two, or three frames. As delay increases, the total number of signal pairs that can be presented across the entire stimulus duration changes. Importantly, however, the total number of possible symmetric pairs with a single frame does not change outside of the limits of the delay. For the 0 ms delay condition, where paired elements were not temporally offset, every frame contains the anticipated number of signal pairs from the beginning of the first frame to the end of the 32nd frame. However, a 40 ms SOA (for example) by necessity means that the first four frames cannot contain signal elements, and symmetry can only be presented from the fifth frame onward. Signal is therefore restricted to

280 ms of the total 320 ms. Control studies conducted in our previous temporal integration publications using the same paradigm have shown that the reduction in the total number of frames containing symmetry signal is very unlikely to contribute to the effects of increasing intra-element delay (Bellagarda et al., 2021; Bellagarda et al., 2022). Although element lifetime, delay duration, and signal to noise ratio was consistent across all experimental conditions, the manner in which temporal delay impacted the overall array depended on the spatial relationships between pairs of elements and is explained independently for each condition.

Stimulus conditions

Five stimulus conditions were included in this experiment. All conditions had a vertical symmetry axis. Four of these conditions were composed of the vertices described above. The relationship of each vertex to the other vertices in the array was varied to manipulate the presence and type of higher-order structure in the array. The fifth condition had no additional higher order structure and contained individual horizontally oriented Gabors. Examples of each condition are shown in Figure 2. These conditions were selected to permit five key comparisons of interest. First, and most pertinently, we ask whether higher-order structure in the form of correlational quadrangles is more salient than patterns defined by either horizontal Gabors or reflected corners alone. This was achieved using the horizontal Gabors, mirrored corners and correlational quadrangles (see Figures 2A,B,D, respectively). Following this, we also asked whether corners need to be reflected across the axis to facilitate perception of the underlying positional symmetry by comparing our reflected and unreflected corners (see Figures 2B,C). Finally, we ask whether the type of higher-order structure in an array is important (see Figures 2B,D,D,E). Does the structure need to span the symmetry axis, as in the correlational quadrangles (see Figures 2B,D), or is reflection of discrete four cornered shapes (see Figures 2D,E) just as readily perceived?

Horizontal gabors

Stimuli in this condition were constructed using individual horizontally oriented Gabor elements (see Figure 2A), similar to those used previously in studies of local orientation in mirror symmetry perception (Bellagarda et al., 2022; Sharman & Gheorghiu, 2019). The Gabors had the same features used in all other conditions, the only difference being that the individual Gabors were not spliced together to create vertices. This condition was included as a baseline to identify variation in symmetry detection arising

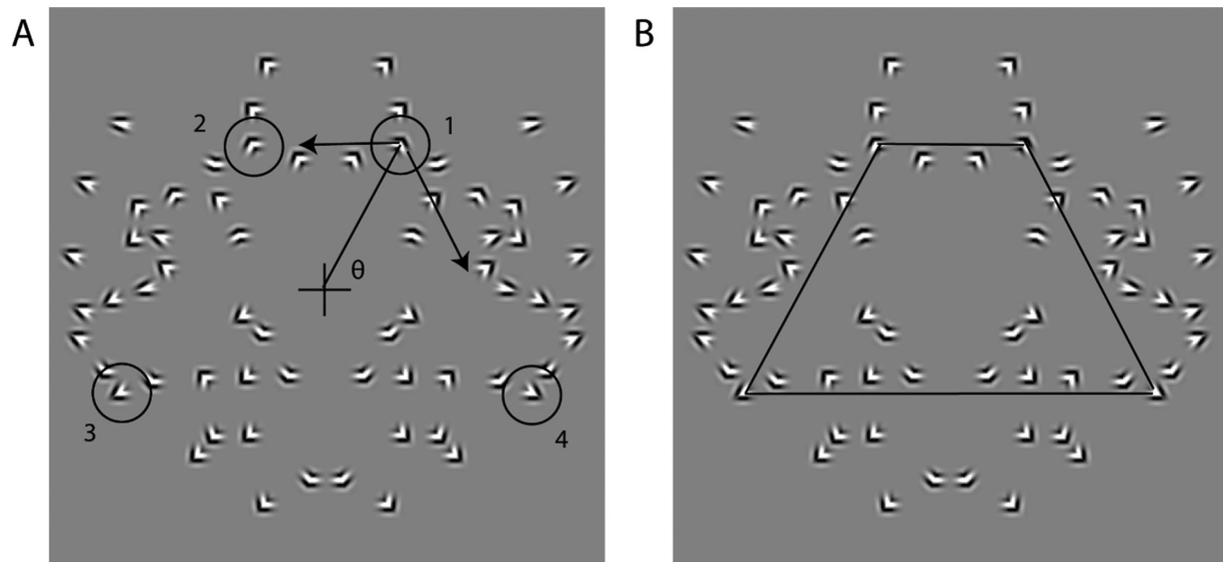


Figure 4. Schematic detailing formation of the correlational quadrangle stimuli. **(A)** Four symmetric positions spanning the symmetry axis are selected, with the symmetry axis as the centroid. With respect to the centroid, the polar angle for each point was calculated. Beginning with point with the smallest polar angle, we determine the angle of the Gabor forming the first leg of the vertex. One leg on each vertex is always oriented horizontally at 90 degrees to the symmetry axis, to align with the horizontal leg of its partner across the axis. The second leg is variably oriented to align with the second leg of the vertex on the same side of the axis. This process continues systematically around the second, third, and fourth largest points to form **(B)** one correlational quadrangle centered on the symmetry axis.

from the vertex elements and additional structure provided by the shapes, compared to more standard Gabor elements containing a narrow orientation range. Symmetry in this case was thus defined by collinear pairs of horizontal Gabors falling on a horizontal virtual line that are independent of all other pairs in the array, similar to the mirrored and unmirrored corners conditions, described below. This condition is identical to our study of local orientation information in symmetry perception (Bellagarda, Dickinson, Bell, & Badcock, 2022). Two participants (CB and ED) completed both studies in parallel, and their data are used in both this experiment and in Bellagarda et al. (2022). The other (TM and MF) participants completed only the conditions of this experiment.

Correlational quadrangles

In the correlational quadrangles condition (see Figure 2D), signal is defined by a higher structure created from four vertices forming a four-sided polygon. In this case, the shape extends across the symmetry axis such that the centroid is always on the symmetry axis. As in the mirrored corners condition, each vertex has one horizontal edge oriented orthogonal to the axis of symmetry, coaligned with the horizontal edge of the symmetrically positioned vertex across the axis. The angle of the second edge within an element varies but is always oriented at the angle required to co-align with

the second edge of another vertex on the same side of the axis. This means that trajectory of the virtual lines created by a vertex is the same as two other vertices in the array, one orthogonal to the axis and the other parallel. In essence, each correlational quadrangle is formed by a “pair of pairs” extending across the axis. This process is shown in Figure 4. Signal levels of four, eight, 12, 16, 20, 24, 28, or 32 pairs of symmetrically positioned vertices correspond to two, four, six, eight, 10, 12, 14, or 16 correlational quadrangles respectively (Signal level/2).

Mirrored corners

In the mirrored corners condition (see Figure 2B), symmetry is defined by low-level collinearity where pairs of vertices are reflected over the central axis. They are formed from the correlational quadrangles condition described above, but the alignment of pairs of elements is disrupted to inhibit higher-order structure. All vertices in the array contain one horizontal edge positioned orthogonal to the symmetry axis. The second edge of each vertex could be at any angle relative to the horizontal edge. Whereas the angle of the second edge is mirrored across the axis, it is angled such that no two vertices are aligned on the same side of the axis. For paired elements, both vertices have the same position and internal angle, such that they are mirrored over the midline. Noise elements are not paired over the axis,

and the second edge of each vertex is oriented such that it is not coincident with any other part of the array. The orientation of the second edge of the vertex is defined by first forming a correlational quadrangle, as described above, and then rotating the two collinear edges on the left side by $\pi/8$ (22.5 degrees anti-clockwise) and those on the right side by $-\pi/8$ (22.5 degrees clockwise). This disrupts the correlational quadrangle, but results in the

signal vertices on the left and right being mirror images of each other. Signal in this case is defined by spatially coincident pairs of vertices, and all features (including position, orientation, and internal angle) are maintained in mirrored form across the axis. Furthermore, the projected and virtual lines between paired elements are indicated by the co-aligned horizontal edge of each angle.

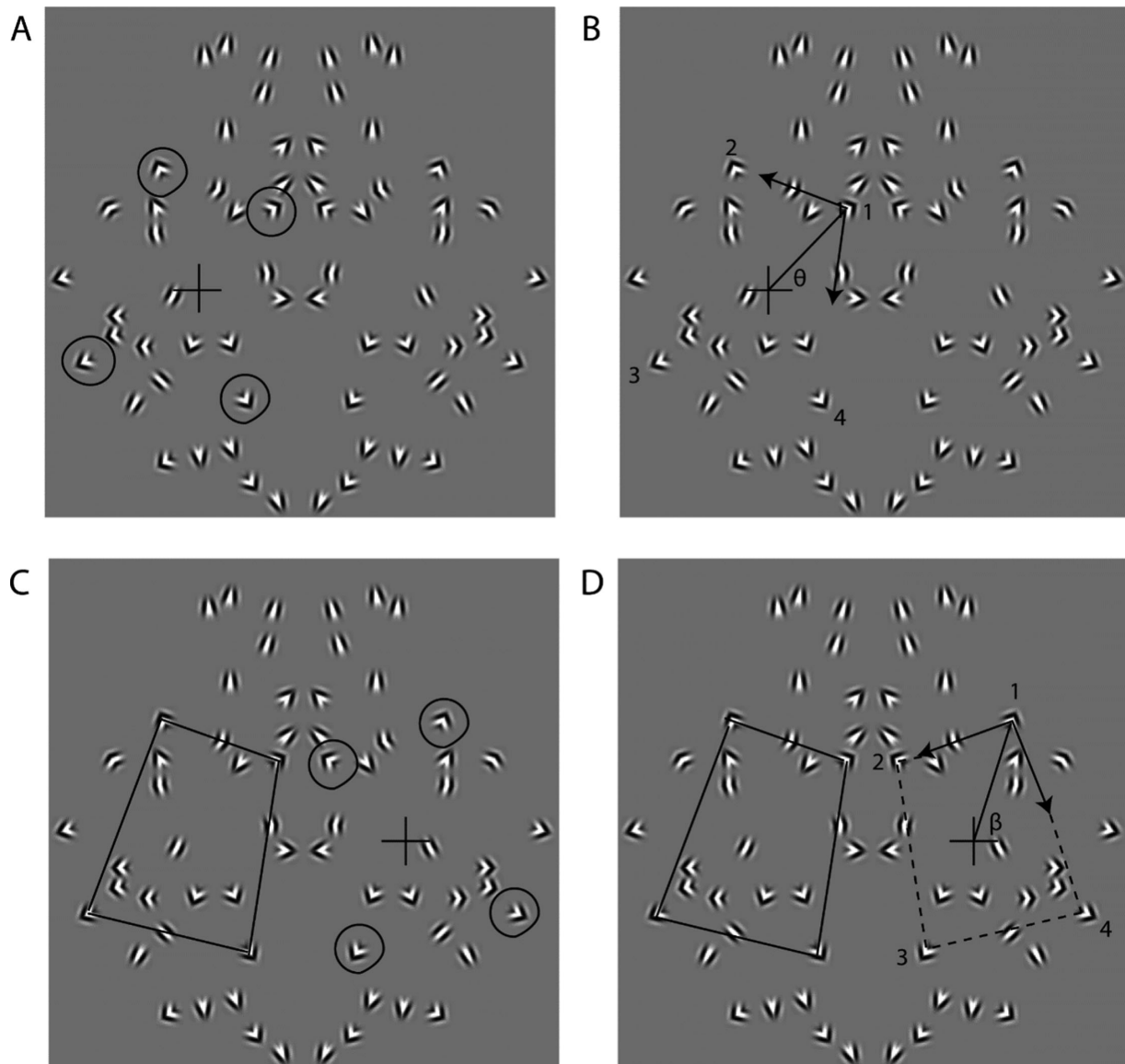


Figure 5. To form the signal shapes, (A) four signal positions are selected on the left side of the symmetry axis. The mean of the positions of the four points was calculated in the X and Y dimensions to determine the location of the shape's centroid. (B) With respect to the centroid, the polar angle for each point was calculated and then ordered by magnitude from smallest to largest. Beginning with the point with the smallest polar angle, we determined the angle of the Gabor forming the first edge of a vertex. This was aligned toward the position with the next largest polar angle. The second edge was oriented towards the last position forming the vertex defining the first corner. The second, third, and fourth corners were treated similarly in turn forming the shape. (C) The corresponding mirror reflection of this shape was generated in the same manner on the other side of the axis by (D) choosing the same four positions. Noise shapes were also generated in the same way, but without the corresponding shape across the axis.

Mirrored shapes

Here, symmetry is defined by the mirror reflection of an otherwise abstract four-cornered shape over the axis of symmetry (see [Figure 2E](#)). The process by which the shape stimuli were formed is detailed in [Figure 5](#). The more shapes that are reflected in this manner, the stronger the symmetry signal. Signal levels of four, eight, 12, 16, 20, 24, 28, or 32 pairs of symmetrically positioned vertices correspond to one, two, three, four, five, six, seven, or eight shapes respectively (Signal level/4). Noise is also defined by a four-cornered polygon, but they are not reflected over the axis; that is, a congruent shape occurs on the left compared to the shape on the right.

Delay is implemented in the same manner as described above by delaying the onset of the elements on one side of the axis relative to the other. However, because symmetry signal in this condition was defined by groups of four elements, all four need to be present on screen for the same four frame lifetime. The second group of four elements on the other side of the axis also appeared together on the delayed frame and existed on screen for the subsequent four frames. This was necessary to maintain the intended signal to noise ratio from frame to frame. As a result, on some frames no elements would be removed and replaced, but on others a group of four elements will be replaced simultaneously. Noise elements change in the same manner. The signal to noise ratio remains constant for each frame of a particular stimulus. The sudden onset of a group of elements may have made the groups easier to detect ([Blake, 1999](#); [Lee & Blake, 2001](#); [Rideaux, Badcock, Johnston, & Edwards, 2016](#)) but this effect was the same for both signal and noise stimuli. Differences between the correlational quadrangle and mirrored shapes stimuli are illustrated in [Figure 6](#).

Unmirrored corners

In the unmirrored corners signal stimuli (see [Figure 2C](#)), only the position of the apex of the vertices is symmetrically placed. The orientation of both edges and the internal angle of each vertex is maintained both between and within pairs, but the entire corner is rotated around its own central apex. The stimuli were constructed by creating a mirrored shapes stimulus as described above and then rotating all vertices by $\pi/8$ (22.5 degrees anticlockwise) disrupting the shapes and ensuring that the signal vertices on the right were rotated by $\pi/4$ (45 degrees) with respect to the mirror image of their partner on the left. The same process was conducted for the noise vertices, except these elements did not have symmetrically corresponding apex locations.

Task

Four participants completed all five experimental conditions. The five experimental conditions were randomly interleaved in a different order for each participant, such that all runs were completed for a given condition before the participant moved to the next. Each participant completed two runs of 120 trials for each delay duration and shape condition. Each participant therefore completed 11,200 trials. Twenty trials were completed for each MOCS step. A two-interval forced-choice task was used. Trials were composed of a test stimulus containing a proportion of symmetric pairs, and an all noise (asymmetric) reference stimulus. Individual stimuli were presented for 320 ms, with a 700 ms ISI between successive stimuli (i.e. the required time to generate the next stimulus).

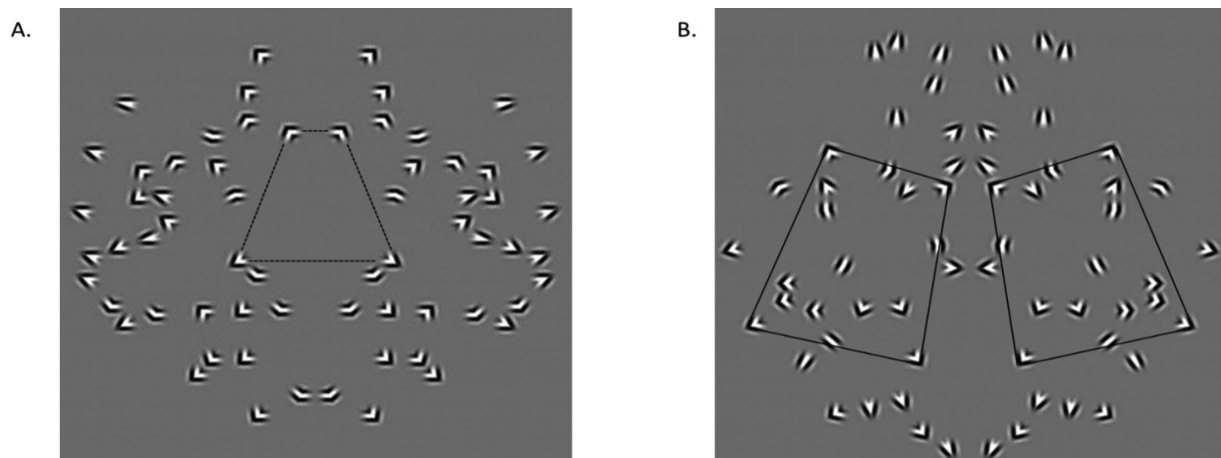


Figure 6. Examples of the different types of higher-order structure used in this experiment. Some of the virtual lines between grouped elements have been drawn on in this example to highlight difference in structure between the two types of stimuli, but were not included on the stimuli used in the experiment. In **(A)** the correlation quadrangles, structure is formed by four symmetrically positioned corners forming a single shape that spans the symmetry axis. Conversely in **(B)** the reflected shapes the condition, the group of four corners is reflected over the axis to form two discrete but mirrored polygons on either side of the array.

Participants indicated whether the first or second interval contained the symmetric stimulus using the top left and right buttons of a CRS, CB6 button box.

Results

The mean proportion of correct responses was calculated for each combination of the eight MOCS steps, seven delay durations and five experimental conditions. Data sets for individual participants were inspected, and a similar pattern of performance was identified across all four participants. As a result, we have elected to average performance prior to further analyses to maintain consistency with our previous studies. A Quick function (Quick, 1974) was fit to the data describing proportion correct versus signal level to estimate the signal level (proportion of symmetrically

positioned element pairs) required to correctly identify the symmetric interval on 75% of trials. Note that thresholds for the two conditions containing higher-order structure (correlational quadrangles and reflected shapes) could also be calculated based on the number of quadrangles or shapes present in a stimulus. To allow for more straightforward comparison between patterns with higher- versus lower-order structure, thresholds will be reported as a percentage of symmetrically positioned pairs. The percentage of symmetrically positioned elements was calculated for the psychometric functions fit to the number of symmetry pairs in all cases.

As is evident in Figure 7, all five conditions are observed to have a similar functional form and show a consistent upper limit to temporal integration. Although each condition appears to change in a similar manner with increasing delay, there is a substantial vertical separation between conditions. This suggests a

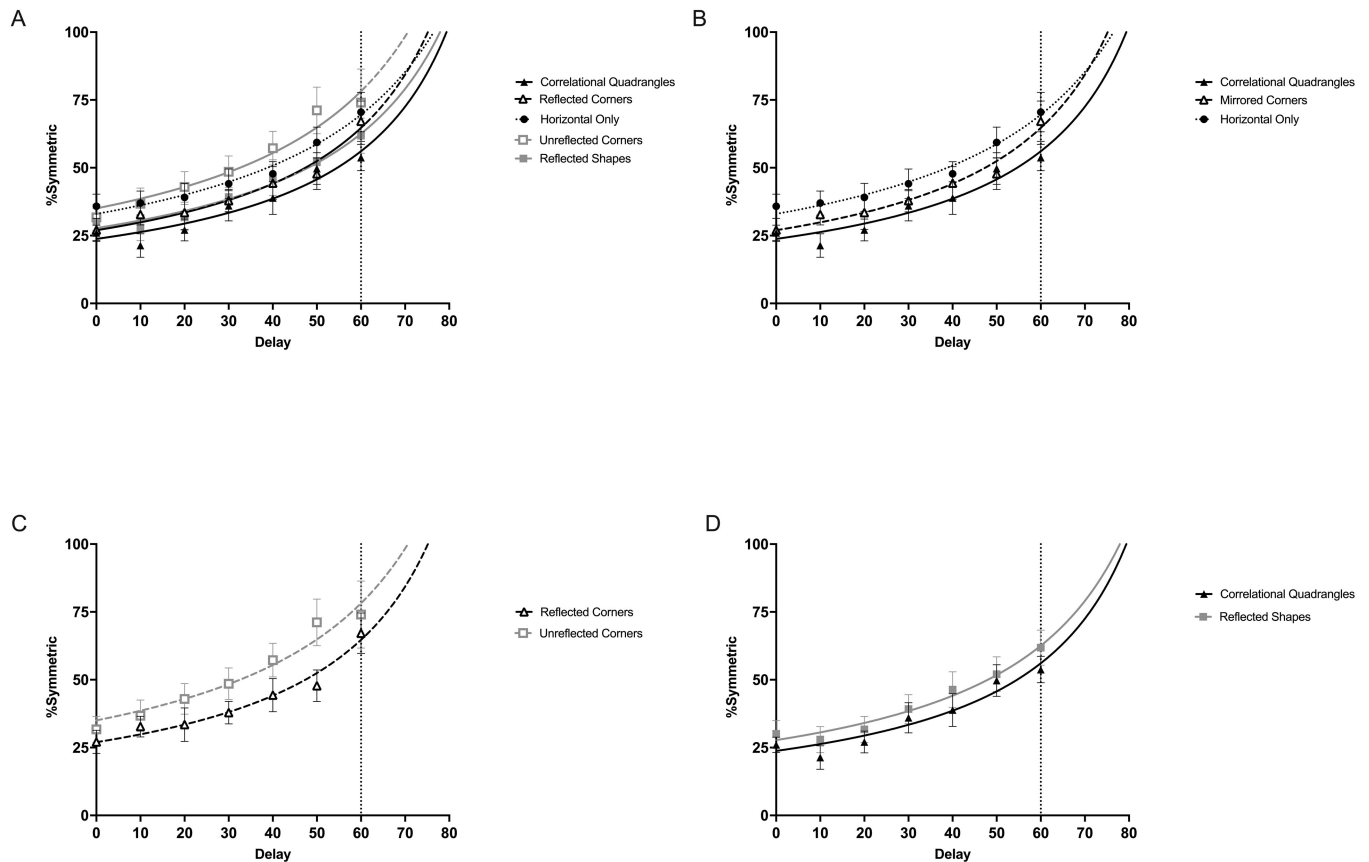


Figure 7. Thresholds and model fits for the five stimulus conditions used in this experiment across each of the seven delay durations. Mean 75% correct thresholds across four participants are plotted for each SOA with accompanying 95% confidence intervals. Each condition is then fit with the two-parameter fit function. Conditions where higher-order structure are shown with solid lines, whereas conditions defined by lower-order information only are shown with broken lines. Panel (A) includes all five conditions, and highlights the significant vertical separation between most conditions. Graphs are then split into our three comparisons of interest which are discussed in more detail below; (B) horizontal only, reflected corners and correlational quadrangles, (C) reflected versus unreflected corners, and (D) correlation quadrangles compared to mirrored shapes. In all panels, the axis has been extended to show where greater than 100% signal is required.

	Horizontal only	Mirrored corners	Correlational quadrangles	Unmirrored corners	Mirrored shapes
Threshold (T_0)	10.56 (33%)	8.64 (27%)	7.61 (24%)	11.21 (35%)	8.89 (28%)
Threshold (T_0) 95% CI	9.75 to 11.42	7.63 to 9.72	6.35 to 9.01	9.8 to 12.74	8.05 to 9.77
Persistence (P)	74.17	62.92	64.14	68.71	67.87
Persistence (P) 95% CI	63.70 to 88.99	52.10 to 80.05	49.40 to 93.15	55.18 to 91.81	57.51 to 83.15
R squared	0.98	0.97	0.93	0.95	0.97

Table 1. Characteristics of integration curves for each condition. *Thresholds = number of symmetric pairs (percent symmetric), persistence = ms SOA. CI = 95% confidence interval.

difference in sensitivity depending on element type, as well as the presence and type of higher-order structure in a given pattern. To obtain a more nuanced analysis of sensitivity to and processing of mirror symmetry in each condition, we applied a two-parameter fit model used in our previous studies of temporal integration mirror symmetry (Bellagarda et al., 2021). The two-parameter fit function uses estimated threshold (T_0) and persistence (P) as free parameters, along with delay duration as an independent variable and the 40 ms element lifetime (L), thus leading to the function:

$$threshold = T_0 \left(\frac{L + P}{L + P - delay} \right).$$

The function works from the hypothesis that although all elements are physically presented on the screen for 40 ms (lifetime, or L), their signal continues to persist as signal to the visual system for a variable duration after the end of this physical lifetime (Badcock & Lovegrove, 1981; Coltheart, 1980; Niimi et al., 2005). We refer to this as persistence, or P. Therefore, the total duration over which an element can act as signal to the visual system is $L + P$, or the sum of physical lifetime plus visible persistence. Because L is always fixed at 40 ms, we only report values for P as the estimated duration *after* this physical lifetime ends. It should be noted that P estimates the duration over which signal can be distributed while still acting as signal to the visual system. A shorter P indicates lower tolerance of temporal delay, and a small T_0 indicates lower symmetry detection thresholds. These values are summarized in Table 1. Examining these results, we can see a high proportion of the variance across the five conditions is explained by the model (mean R^2 value = 96%). Model fits were compared across conditions using an extra sum of squares F test (Motulsky, 2007), showing significant differences in processing across the five conditions; $F(8, 25) = 15.69, p < 0.0001, \eta_p^2 = 0.83$. This is driven by a significant difference in T_0 across conditions; $F(4, 25) = 11.04, p < 0.001, \eta_p^2 = 0.64$. There was no significant difference between P estimates; $F(4, 25) = .49, p = 0.74, \eta_p^2 = 0.07$. As P does not change across conditions, our subsequent analyses will focus on T_0 . Conditions are compared independently with Bonferroni correction; as seven comparisons are reported here, the significant

level used following correction was 0.007 (0.05/7). Here, individual extra sums of squares F tests were used to quantify specific differences between T_0 based on the presence and type of higher-order structure in relation to our hypotheses. Note that the below comparisons were planned prior to completion of the study. However, we will only report comparisons between T_0 estimates, which were identified as driving the significant differences in the above comparisons.

Is there a role for higher-order structure in mirror symmetry perception?

In all our conditions, symmetric pairs are defined by elements falling along the same virtual line oriented orthogonal to the symmetry axis. Previous work (Bellagarda et al., 2022; Saarinen & Levi, 2000) typically shows horizontal elements, that are also oriented orthogonally to the symmetry axis like the virtual line they fall on, make a strong contribution to symmetry detection mechanisms. In the mirrored corners condition, the horizontal component is preserved in these elements with the same features as the horizontal only condition. The difference between the two conditions is the addition of a second leg in the mirrored corner elements, which does not fall along this virtual line and contains an additional projected line. If the additional orientation information in the mirrored corners condition is disruptive to mirror symmetry, we would expect to see higher T_0 estimates in the mirrored corners compared to the horizontal only elements. T_0 was significantly lower in the mirrored corners condition compared to the horizontal only condition ($F(1, 10) = 13.47, p = 0.002, \eta_p^2 = 0.57$). This indicates that not only are corner elements containing two orientation components not disruptive to symmetry detection, but our participants were more sensitive to symmetry in this condition than when patterns were composed of horizontal Gabors.

We turn now to the main question of interest for this paper; are patterns with higher-order structure more readily detected than patterns with only lower-order structure? In the case of the reflected corners condition, higher-order structure is specifically weakened by manipulation of the alignment of the vertices so

that no additional concordant projected lines can be formed by component elements other than those defining the bilateral symmetry. Higher-order structure, introduced by explicit groupings of pairs of elements into four-cornered shapes spanning the symmetry axis, should introduce additional structural information into the symmetry array that cannot be achieved in non-symmetric reference patterns. The additional structure in correlational quadrangle stimuli leads to better symmetry detection performance than for conditions where symmetry is described by position alone, indicated by significantly lower T_0 in the correlational quadrangle condition (horizontal only $F(1, 10) = 22.12, p < 0.001, \eta_p^2 = 0.69$; unreflected corners $F(1, 10) = 21.01, p < 0.001, \eta_p^2 = 0.68$). However, T_0 for the reflected corners condition does not differ from the correlational quadrangles condition ($F(1, 10) = 2.4, p = 0.08, \eta_p^2 = 0.19$). The only difference between these two conditions is the orientation of the second leg of each vertex. In the correlational quadrangle, this leg is angled to align with the second leg of another vertex on the same side of the axis, creating the higher-order structure. In the reflected corners condition, this leg is oriented such that it does *not* align with the second leg of any other vertex in the array. In both cases, the first leg of a given vertex is always horizontal, and always aligns with the first horizontal leg of its symmetrically positioned corner element across the axis. These horizontal projected lines will fall along the existing position based horizontal virtual line across the axis. Patterns where component elements form correlational quadrangles are more readily detected than patterns with any variation of higher-order structure considered thus far. Although this is small for the reflected corners condition, the additional structure added by the presence of correlational quadrangles does make a contribution to sensitivity here.

Do nonreflected corner elements disrupt symmetry detection?

In both the horizontal only and mirrored corners condition, the position and identity of elements are always reflected over the symmetry axis. Previous research has shown that when symmetric pairs are composed of oriented elements that are not reflected over the axis, such as if one element is horizontal while the other is vertical, both T_0 and P estimates are significantly higher than when paired elements are reflected (e.g. two horizontal or two vertical Gabors; Bellagarda et al., 2022). Other studies have also shown a significantly disruptive effect of mismatching Gabor elements within pairs, both in terms of orientation (Saarinen & Levi, 2000) and other features such as luminance polarity (Bellagarda et al., 2021; Wenderoth,

1996; Zhang & Gerbino, 1992). Based on these findings, it is sensible to consider whether a similar effect may occur if corner elements are not reflected over the axis. Here, the apex of both corners will fall in mirrored positions across the axis, however the orientation of the internal angle of the elements will not be reflected across the axis. Based on previous studies, it can be hypothesized that unmirrored corner elements will have a detrimental effect on symmetry perception compared to either horizontal Gabor elements, or reflected corner elements.

Compared to reflected corners, the unreflected corners have a large significant disruptive effect as T_0 for unreflected corners was significantly higher ($F(1, 10) = 13.03, p = 0.003, \eta_p^2 = 0.57$). However, this sensitivity cost is quite small when comparing with horizontal Gabors. There was no significant difference in T_0 between horizontal only and unreflected corners ($F(1, 10) = 0.93, p = 0.18, \eta_p^2 = 0.09$). This is contrary to expectations given the disruptive effects of mismatching element orientation in previous studies (Bellagarda et al., 2022). From this, we would expect a significant detrimental effect of unmirrored corners compared to both the horizontal only and mirrored corners conditions as neither should interfere with low-level positional information as is expected from the unmirrored corners condition. This result implies that the visual system can reconcile discordant information from non-symmetric vertices in symmetric positions, but it also shows that useful information is added by the second leg of the mirrored corners additional to the existing horizontal information present in Gabor elements. The benefit of additional information from mirrored corners, which reinforce virtual lines, appears greater than the cost introduced by unmirrored corners, which was expected to disrupt symmetry signal. The most relevant finding for our experiment, however, is that detection of symmetry in patterns composed of corners is the same or better than patterns with traditional Gabor elements containing a very narrow range of orientations.

Does type of higher-order structure matter in symmetry detection?

The reflected shapes condition is formed by grouping four corner elements on one side of the axis, and reflecting this group of four across the axis to form two mirror symmetric four cornered polygons. Rather than spanning the symmetry axis, structure here is formed from mirror reflection of two separate abstract shapes on either side. Both types of structure are embedded in an intrinsically symmetrical array, but can be conceptualized as a one- versus two-object problem (Baylis & Driver, 2001; Koning & Wagemans, 2009). This is highlighted in Figure 6 below. If the benefit of

corner elements, and the introduction of higher-order structure spanning the central axis, is that it makes the symmetry information more readily perceptible by strengthening lower-order pairwise structure, then we would expect that our correlational quadrangle stimuli would be more salient than our reflected shapes condition. The reflected shapes condition does introduce additional structural information to the symmetric pattern. However, it also introduces an additional computational step of comparing discrete four cornered shapes over the axis to determine whether they are symmetric which is shown to negatively impact symmetry in studies using solid polygons (Baylis & Driver, 2001; Bertamini, 2010; Koning & Wagemans, 2009).

Directly comparing the two higher order structure conditions with each other would provide more direct support for this hypothesis. Reflected shapes was found to require approximately 4% more symmetry signal than the correlational quadrangles condition (see Table 1). When T_0 is compared in isolation, they are not-significantly different ($F(1, 10) = 4.21$, $p = 0.035$, $\eta_p^2 = 0.30$). However, this does not negate the observation of a small benefit of higher-order structure in symmetry.

Discussion

Taken as a whole, our findings support the role of higher order structure in strengthening mirror symmetry perception, replicating, and extending earlier findings by Wagemans et al. (1993). We also show that structure throughout the entire pattern makes a small but meaningful contribution to symmetry detection compared to the additional of isolated symmetric sub-components, consistent with previous studies using solid shapes (Baylis & Driver, 2001; Bertamini, 2010; Koning & Wagemans, 2009). The stimulus properties leading to the percept of visual mirror symmetry arguably exist at the intersection of local element interactions and global pattern recognition. Although symmetry itself is a high-level feature, it is strongly dependent on very precise arrangements of discrete local information, and disruption at either level can have significant negative effects on the salience of a given pattern (Jenkins, 1983). Wagemans et al. (1993) bootstrapping model of symmetry perception emphasizes the role of higher-order structure in symmetry perception, and posits that this intersection of low-level pairs and global symmetry bridges the gap in conceptualization of symmetry perception at the intersection of local-global processing. However, investigation of Wagemans et al.'s model was restricted by using dot or Gabor patterns, which limits how much interaction between- and within-pairs can be

manipulated. Recent research by (Persike & Meinhardt, 2016; Persike & Meinhardt, 2017) introduces concept of corner elements, composed of two orientation components joined along a central point to form corners of varying internal angles. Compared to dot elements, which are non-oriented, and Gabors or lines, which are predominately a single orientation, the two orientation components in each corner creates two projected lines in different directions and thus relationships between symmetric pairs can be dictated by features beyond spatial position alone. The overarching aim of the current study was to provide a systematic investigation of the role of higher-order structure in visual mirror symmetry, as suggested in the bootstrapping model, using stimuli composed of corner elements where the presence and type of structure could be manipulated explicitly, to expand on Wagemans et al. (1993) findings using dot patterns.

The current study has two complementary main findings. Expanding on (Persike & Meinhardt, 2016; Persike & Meinhardt, 2017) contour integration research, we show that corner elements can make an important contribution to investigations of mirror symmetry perception. We show that symmetry is detectable in patterns solely composed of corner elements, and that detection thresholds (T_0) vary only slightly from patterns composed solely of horizontal Gabor elements. Interestingly, this similarity in processing is retained when comparing mirrored and unmirrored corners, which seems contrary to research with Gabor elements where mismatching across the axis has very large negative consequences for global pattern perception (Saarinen & Levi, 2000). In this case, it may be that the visual system is discarding irrelevant orientation components and using the convergence of information at the apex. The apex of the corner is in the same symmetrical position as its partner regardless of orientation and falls in the same point as the midpoint of a Gabor element. Some researchers have argued that this midpoint is the core piece of information used in symmetry processing, and variations in orientation components may be largely irrelevant (Koepl & Morgan, 1993). However, follow-up research examining local element orientation has shown quite convincingly that this is not the case. Variations in local element orientations significantly impact the salience of the overall pattern, and positional information is not sufficient without concordance of other element features (Bellagarda et al., 2022; Saarinen & Levi, 2000). Our findings with corner elements similarly contradict this assertion when directly comparing results for mirrored versus unmirrored corners conditions. Just as unmirrored elements are still recognizable as symmetric but require more symmetry information, the same is true for corner elements as the mirrored corners condition had significantly lower detection thresholds than the unmirrored corners condition. Overall, this

suggests that while the visual system can reconcile this conflict, this comes with an additional cost in terms of reduced sensitivity (higher T_0). As (Persike & Meinhardt, 2016; Persike & Meinhardt, 2017) had shown previously in their contour integration studies, corner elements can make an important contribution to understanding global form processing, but this is driven by the interaction of these elements rather than an intrinsic difference in processing at the element level. At an element level, we show that corner and Gabor elements produce very similar symmetry detection thresholds. At the pattern level however, employing reflected corner elements allows for greater, more controlled manipulation of inter-element relationships within and between pairs. This is greater than that offered by oriented Gabors or non-oriented dots, particularly for investigating the role of higher-order structure in mirror symmetry.

Consistent with our hypotheses, and with Wagemans et al. (1993) findings, participants were more sensitive to patterns with higher-order structure defined by correlational quadrangles, compared to patterns with lower-order structure alone. Structure spanning the symmetry axis makes a significantly greater contribution to the detectability of the global symmetry, even when compared to patterns with reflected substructures or shapes. This finding is consistent with that of Wagemans et al. (1993) and suggests that the proposed bootstrapping process is facilitated in a “pairs of pairs” arrangement across the symmetry axis. Arguably, the additional structural information in a correlational quadrangle arrangement promotes the pattern as being viewed as a single object. In contrast, the reflected shapes condition leads to the pattern being viewed as a collection of reflected sub-shapes. If we consider research using solid polygons that consistently shows that mirror symmetry is a one-object cue, and mirror symmetry is consistently more salient when present in a single object rather than across two separate objects (Baylis & Driver, 1995; Baylis & Driver, 2001; Bertamini, 2010), this difference is not surprising. Our findings here support and strengthen Wagemans et al. (1993; Wagemans, 1993; Wagemans et al., 1991) assertion that higher-order structure is important in mirror symmetry perception, and bolsters detectability of the global pattern. Higher-order structure might be considered to be in a similar league to other important symmetry features that have been previously identified, such as pattern outline (Wenderoth, 1995) or the central integration region around the symmetry axis (Dakin & Herbert, 1998; Kurki, 2019). The global symmetry of the pattern is still recognizable when any one of these intermediate features are disrupted, but there is a significant cost to observer sensitivity. All of these features can be thought of as promoting ready axis identification and recognition of a symmetric pattern as a single discrete object, therefore

strengthening the relationship between local and global information.

Our evidence for the important role of higher-order structure in symmetry perception is especially interesting when considering existing influential models of symmetry perception. Spatial filter models (Dakin & Watt, 1994; Rainville & Kingdom, 2000) are the most commonly accepted model of mirror symmetry perception. These models are loosely based on Jenkins' (1983) component process model; spatially symmetric elements are processed by the same filter, forming orthogonal blobs stacked along the symmetric axis. The more blobs that are formed, and the greater the degree of co-alignment along the axis, the stronger the symmetry signal. Both first- and second-order filtering mechanisms are implicated in symmetry perception, and the overall model is fairly robust to many variations in local and global symmetry features (Brooks & van der Zwan, 2002; Dakin & Hess, 1997; Rainville & Kingdom, 2000; van der Zwan, Badcock, & Parkin, 1999). However, current spatial filtering models cannot explain the findings of this study. By using a temporal integration paradigm, we can show that processing of symmetry in all five conditions has characteristics of a first-order mechanism; low detection thresholds (T_0) and short persistence (P) values, indicative of a fast but sensitive system (Bellagarda et al., 2021). This is further reinforced by the lack of variability in P estimates across conditions, as this is consistent with processing at points in the visual system with similar temporal sensitivity. In our previous work considering luminance polarity (Bellagarda et al., 2021) and element orientation (Bellagarda et al., 2022), we suggest that P is longer to allow for accumulation of information when the symmetry signal is noisy or disrupted in some way. In these studies, we showed that when elements are not concordant across the midline, such opposite luminance polarities or large orientation variation, symmetry is more difficult to detect (higher T_0 estimate) and the signal persists for longer in the visual system (higher P estimate). One possible explanation for this is that P and T_0 covary, such that a significant increase in T_0 necessitates an increase in P. However, in the current study P does not change significantly, even though we report significant differences in T_0 . For instance, in the unreflected corners condition, where elements are not symmetric over the midline and T_0 significantly increased while P did not. Such results argue against a linear covariation of T_0 and P, and instead suggests that T_0 and P are largely independent of each other. Of course, multiple mechanisms with identical time courses could also be proposed at the cost of parsimony. However, first-order mechanisms are sensitive to variations in element features and cannot account for the difference in sensitivity when corners are reflected or unreflected. As symmetry signal in spatial filtering is defined as the quantity of coaligned

horizontal blobs (Dakin & Watt, 1994; Jenkins, 1983), the formation of higher-order structure is lost. In all stimuli, all symmetrically paired elements produce a mid-point on a virtual line that falls on the same orthogonal virtual line indicating the symmetry axis. Therefore, all five conditions have the same quantity of horizontal virtual lines and thus equivalent symmetry information according to spatial filtering definitions as in all cases symmetric pairs are positioned to stimulate the same horizontal filter. This means that the difference between reflected shapes and correlational quadrangles is also lost, and cannot be accounted for from the currently proposed spatial filtering perspectives.

Our study, in conjunction with earlier findings by Wagemans et al. (1993) cements the importance of higher-order structure in symmetry perception, particularly as a potential way of bridging the gap between local elements and global symmetry. This cannot be captured by widely used spatial filtering models of symmetry perception, and suggests the need for more nuanced, flexible models and stimuli that can account for symmetry perception including both higher- and lower-order information. Some attempts have been made to do this, such as Dry (2008) Voronoi tessellation model, but testing of these are limited by stimulus choices much like Wagemans et al. (1993) original investigations of their bootstrap model using dot elements. The introduction of stimuli such as (Persike & Meinhardt, 2016; Persike & Meinhardt, 2017) corner elements permit a greater level of confidence in the presence and type of higher order structure present, and thus inform the development of more flexible models of symmetry perception capturing a wider range of real-world features.

Keywords: symmetry, structure, corners

Acknowledgments

Supported by Australian Research Council Grants DP160104211 and DP190103474 to D.R.B.

Commercial relationships: none.

Corresponding author: Cayla Bellagarda.

Email: cayla.bellagarda@research.uwa.edu.au.

Address: School of Psychological Science (M304), The University of Western Australia, 35 Stirling Highway, 6009 Crawley, Western Australia.

References

- Badcock, D. R., & Lovegrove, W. (1981). The effects of contrast, stimulus duration, and spatial frequency on visible persistence in normal and specifically disabled readers. *Journal of Experimental Psychology: Human Perception and Performance*, 7(3), 495–505.
- Barlow, H. B. (1985). Cerebral Cortex as Model Builder. In V. D. D. Rose (Ed.), *Models of the Visual Cortex* (pp. 37–46). Hoboken, NJ: John Wiley & Sons.
- Baylis, G. C., & Driver, J. (1995). Obligatory Edge Assignment in Vision: The Role of Figure and Part Segmentation in Symmetry Detection. *Journal of Experimental Psychology: Human Perception and Performance*, 21(6), 1323–1342.
- Baylis, G. C., & Driver, J. (2001). Perception of symmetry and repetition within and across visual shapes: Part-descriptions and object-based attention. *Visual Cognition*, 8(2), 163–196.
- Bellagarda, C. A., Dickinson, J. E., Bell, J., & Badcock, D. R. (2021). Temporal Integration Windows for Visual Mirror Symmetry. *Vision Research*, 188, 184–192.
- Bellagarda, C. A., Dickinson, J. E., Bell, J., & Badcock, D. R. (2022). Selectivity for local orientation information in visual mirror symmetry perception. Retrieved from https://papers.ssrn.com/sol3/papers.cfm?abstract_id=4082424.
- Bertamini, M. (2010). Sensitivity to reflection and translation is modulated by objectness. *Perception*, 39(1), 27–40.
- Blake, R. (1999). Visual form created solely from temporal structure. *Science*, 284(5417), 1165–1168.
- Brooks, A., & van der Zwan, R. (2002). The role of ON- and OFF-channel processing in the detection of bilateral symmetry. *Perception*, 31(9), 1061–1072.
- Cohen, E. H., & Zaidi, Q. (2013). Symmetry in context: salience of mirror symmetry in natural patterns. *Journal of Vision*, 13(6), 22.
- Coltheart, M. (1980). Iconic memory and visible persistence. *Perception and Psychophysics*, 27(3), 183–228.
- Corballis, M. C., & Roldan, C. E. (1975). Detection of symmetry as a function of angular orientation. *Journal of Experimental Psychology: Human Perception and Performance*, 1(3), 221–230.
- Dakin, S. C., & Herbert, A. M. (1998). The spatial region of integration for visual symmetry detection. *Proceedings of the Royal Society of London*, 265, 659–664.
- Dakin, S. C., & Hess, R. (1997). The spatial mechanisms mediating symmetry perception. *Vision Research*, 37(20), 2915–2930.
- Dakin, S. C., & Watt, R. J. (1994). Detection of bilateral symmetry using spatial filters. *Spatial Vision*, 8(4), 393–413.
- Driver, J., Baylis, G. C., & Rafal, R. D. (1992). Preserved figure-ground segregation and symmetry perception in visual neglect. *Nature*, 360(6399), 73–75.

- Dry, M. J. (2008). Using relational structure to detect symmetry: a Voronoi tessellation based model of symmetry perception. *Acta Psychol (Amst)*, 128(1), 75–90.
- Field, D. J., Hayes, A., & Hess, R. F. (1993). Contour integration by the human visual system: Evidence for a local "association field". *Vision Research*, 33(2), 173–193.
- Friedenburg, J. D., & Bertamini, M. (2000). Contour symmetry detection: the influence of axis orientation and number of objects. *Acta Psychologica*, 105, 107–118.
- Gheorghiu, E., Kingdom, F. A. A., Remkes, A., Li, H. O., & Rainville, S. (2016). The role of color and attention-to-color in mirror-symmetry perception. *Sci Rep*, 6, 29287.
- Hogben, J. H., Julesz, B., & Ross, J. (1976). Short Term Memory for Symmetry. *Vision Research*, 16, 861–866.
- Jenkins, B. (1983). Component processes in the perception of bilaterally symmetric dot textures. *Perception and Psychophysics*, 34(5), 433–440.
- Jones, B. C., Little, A. C., Penton-Voak, I. S., Tiddeman, B. P., Burt, D. M., & Perrett, D. I. (2001). Facial symmetry and judgements of apparent health: Support for a "good genes" explanation of the attractiveness–symmetry relationship. *Evolution and Human Behaviour*, 22, 417–429.
- Julesz, B. (1971). *Foundations of Cyclopean Vision*. Chicago, Illinois: University of Chicago Press.
- Koepl, U., & Morgan, M. (1993). Local orientation versus local position as determinants of perceived symmetry. *Perception*, 22(Suppl.), 111.
- Koning, A., & Wagemans, J. (2009). Detection of Symmetry and Repetition in One and Two Objects: Structures Versus Strategies. *Experimental Psychology*, 56(1), 5–17.
- Kurki, I. (2019). Stimulus information supporting bilateral symmetry perception. *Vision Res*, 161, 18–24.
- Lee, S. H., & Blake, R. (2001). Neural synergy in visual grouping: When good continuation meets common fate. *Vision Research*, 41(16), 2057–2064.
- Li, W., & Gilbert, C. D. (2002). Global Contour Saliency and Local Colinear Interactions. *Journal of Neurophysiology*, 8(5), 2846–2856.
- Locher, P. J., & Nodine, C. (1989). The perceptual value of symmetry. *Computers & Mathematics with Applications*, 17(4–6), 475–484.
- Locher, P. J., & Wagemans, J. (1993). Effects of element types and spatial grouping on symmetry detection. *Perception*, 22, 565–587.
- Machilsen, B., Pauwels, M., & Wagemans, J. (2009). The role of vertical mirror symmetry in visual shape detection. *Journal of Vision*, 9(12), 11.
- Makin, A. D. J., Rampone, G., Karakashevska, E., & Bertamini, M. (2020). The extrastriate symmetry response can be elicited by flowers and landscapes as well as abstract shapes. *Journal of Vision*, 20(5), 11.
- Mancini, S., Sally, S. L., & Gurnsey, R. (2005). Detection of symmetry and anti-symmetry. *Vision Research*, 45(16), 2145–2160.
- Moor, D. J. H., & Parker, D. J. (1974). Analysis of global pattern features. *Pattern Recognition*, 6, 149–164.
- Morales, D., & Pashler, H. (1999). No role for colour in symmetry perception. *Nature*, 399, 115–116.
- Motulsky, H. J. (2007). *Prism 5 Statistics Guide*. San Diego CA: GraphPad Software Inc.
- Niimi, R., Watanabe, K., & Yokosawa, K. (2005). The role of visible persistence for perception of visual bilateral symmetry. *Japanese Psychological Research*, 47(4), 262–270.
- Pashler, H. (1990). Coordinate Frame for Symmetry Detection and Object Recognition. *Journal of Experimental Psychology: Human Perception and Performance*, 16(1), 150–163.
- Persike, M., & Meinhardt, G. (2016). Contour integration with corners. *Vision Research*, 127, 132–140.
- Persike, M., & Meinhardt, G. (2017). A new angle on contour integration: The role of corners. *Journal of Vision*, 17(12), 9.
- Quick, R. F. (1974). A Vector-Magnitude Model of Contrast Detection. *Kybernetik*, 16, 65–67.
- Rainville, S. J., & Kingdom, F. A. (2000). The functional role of oriented spatial filters in the perception of mirror symmetry — psychophysics and modeling. *Vision Research*, 40, 2621–2644.
- Rideaux, R., Badcock, D. R., Johnston, A., & Edwards, M. (2016). Temporal synchrony is an effective cue for grouping and segmentation in the absence of form cues. *Journal of Vision*, 16(11), 23.
- Saarinen, J., & Levi, D. M. (2000). Perception of mirror symmetry reveals long-range interactions between orientation-selective cortical filters. *NeuroReport*, 11(10), 2133–2138.
- Sawada, T., & Pizlo, Z. (2008). Detection of skewed symmetry. *Journal of Vision*, 8(5): 14, 11–18.
- Sharman, R. J., & Gheorghiu, E. (2019). Orientation of pattern elements does not influence mirror symmetry perception. *Paper presented at the Vision Science Society Annual Meeting Abstract*, Florida. 19(10), 151c.

- Sharman, R. J., Gregersen, S., & Gheorghiu, E. (2018). Temporal dynamics of mirror-symmetry perception. *Journal of Vision*, 18(5), 10.
- Simmons, L. W., Rhodes, G., Peters, M., & Koehler, N. (2004). Are human preferences for facial symmetry focused on signals of developmental instability?. *Behavioral Ecology*, 15(5), 864–871.
- Tan, K. W. S., Dickinson, J. E., & Badcock, D. R. (2016). In unison: First- and second-order information combine for integration of shape information. *Journal of Vision*, 16(11), 9.
- Treder, M. (2010). Behind the Looking-Glass: A Review on Human Symmetry Perception. *Symmetry*, 2(3), 1510–1543.
- Treder, M., van der Vloed, G., & van der Helm, P. A. (2011). Interactions between constituent single symmetries in multiple symmetry. *Attention, Perception Psychophysics*, 73(5), 1487–1502.
- van der Zwan, R., Badcock, D. R., & Parkin, B. (1999). Global form perception: interactions between luminance and texture information. *Australian and New Zealand Journal of Ophthalmology*, 27, 268–270.
- Wagemans, J. (1993). Skewed Symmetry: A Non Accidental Property Used to Perceive Visual Forms. *Journal of Experimental Psychology: Human Perception and Performance*, 19(2), 364–380.
- Wagemans, J., Gool, L. V., Swinnen, V., & Horebeek, J. V. (1993). Higher order structure in regularity detection. *Vision Research*, 33(8), 1067–1088.
- Wagemans, J., van Gool, L., & d’Ydewalle, G. (1991). Detection of symmetry in tachistoscopically presented dot patterns: Effects of symmetry axes and skewing. *Perception and Psychophysics*, 50(5), 413–427.
- Wenderoth, P. (1995). The role of pattern outline in bilateral symmetry detection with briefly flashed dot patterns. *Spatial Vision*, 9(1), 57–77.
- Wenderoth, P. (1996). The effects of the contrast polarity of dot-pair partners on the detection of bilateral symmetry. *Perception*, 25, 757–771.
- Zhang, L., & Gerbino, W. (1992). Symmetry in opposite contrast dot patterns. *Spatial Vision*, 21(Supplement 2), 95.